Supporting Information for

A hierarchical Fe/ZSM-5 zeolite with superior catalytic performance for benzene hydroxylation to phenol

Hongchuan Xin,[a] Arjan Koekkoek,[b] Qihua Yang,[a] Rutger van Santen,[b] Can Li,*[a] and Emiel J.M. Hensen*[b]

[a] State Key Laboratory of Catalysis, Dalian Institute of Chemical Physics, Chinese Academy of Sciences, 457 Zhongshan Road, Dalian, China. Fax: +86-411-84694447; Tel: +86-411-84379070; E-mail: canli@dicp.ac.cn

[b] Schuit Institute of Catalysis, Eindhoven University of Technology, P.O. Box 513, 5600 MB Eindhoven, The Netherlands. Fax: +31-40-2455054; Tel: +31-40-2475178; E-mail: e.j.m.hensen@tue.nl

Experimental Details

Synthesis of materials

A hierarchical Fe/ZSM-5 was hydrothermally synthesized with [3-(trimethoxysilyl)propyl] octadecyldimethylammonium chloride (TPOAC, Acros, 60 wt.% in methanol) as a mesoporogen. In a typical procedure, 4.14 g of TPOAC, 2.66 g of tetrapropylammonium bromide (TPABr, Acros, 98%), and 0.77 g of NaOH were completely dissolved in 36.3 g of H_2O and mixed with 83.3 g of diluted sodium silicate solution (Si/Na = 1.75; 6.83 wt.% SiO_2). A solution containing 0.23 g of sodium aluminate (53 wt.% Al_2O_3, 43 wt.% Na_2O), 0.21 g of $Fe(NO_3)_3 \cdot 9H_2O$ and 26.6 g of H_2O was added dropwise under stirring to the resultant mixture. Subsequently, 26 g of 10 wt.% H_2SO_4 solution was added to the synthesis mixture under vigorous stirring. The final molar composition of the mixture was $Al_2O_3/Fe_2O_3/Na_2O/SiO_2/TPABr/H_2SO_4/H_2O/TPOAC$ = 1.2/0.26/40/95/10/26/9000/5. The mixture was heated at 150 °C for 4 days in a Teflon-coated stainless-steel autoclave. The precipitated product was filtered by suction and washed with distilled water. The as-synthesized sample (mesoFe/ZSM-5-as) was then extracted with methanol under refluxing for 12 h to remove traces of physically occluded silane surfactants. The extracted sample (mesoFe/ZSM-5-ex) was dried in an oven at 100 °C and subsequently calcined in 100 mL min^{-1} N_2 during heating to 550 °C at a ramp rate of 1 °C min^{-1} kept at 550 °C for 8 h, and then further treated in 100 mL min^{-1} 20 vol.% O_2 in N_2 at 550 °C for 4 h. The sample was ion-exchanged into the NH_4^+ form by repeating the ion-exchange treatment three times with a 1 M aqueous solution of NH_4NO_3 at 80 °C for 4 h. The zeolite was calcined in static air at 550 °C for 4 h to convert it to the H^+ form. The sample is named mesoFe/ZSM-5-E. Steam activation was achieved by steaming 1.0 g of mesoFe/ZSM-5-E in a flow of 100 mL min^{-1} 20 vol.% O_2 in N_2 with 10 vol.% water vapor at 700 °C for 3 h. The sample modified by steaming is denoted by mesoFe/ZSM-5-ES. For comparison, the corresponding samples which are calcined and steamed without the extraction step are denoted by mesoFe/ZSM-5-cal and mesoFe/ZSM-5-S, respectively. The synthesis pathway is shown schematically as in Scheme S1.

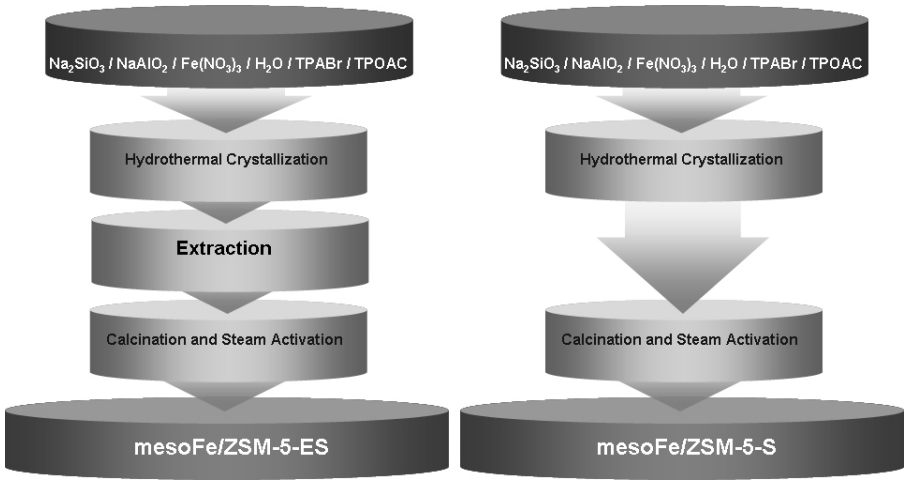

Scheme S1. Schematic illustration of the hydrothermal synthesis routes.

For comparison, Fe/ZSM-5 was prepared by controlled hydrolysis of tetraethylorthosilicate (TEOS, Merck, 98%) in the presence of tetrapropylammonium hydroxide (TPAOH, Merck, 40 wt.% in water) according to a reported procedure.[1] The same calcination and steaming treatments of the as-synthesized sample (Fe/ZSM-5-as) were used as for mesoFe/ZSM-5. The calcined and steamed samples are denoted by Fe/ZSM-5-cal and Fe/ZSM-5-S, respectively.

Characterization

The Fe and Al contents of the calcined zeolites were determined by inductively coupled plasma optical emission spectrometry (ICP-OES) after an aliquot of the sample was dissolved in a mixture of HF and HNO_3. The analyses were performed with a Spectro CIROSCCD spectrometer equipped with a free-running 27.12 MHz generator at 1400 W.

UV-Vis spectra were recorded on a Shimadzu UV-2401 PC spectrometer in diffuse-reflectance mode with a 60 mm integrating sphere. $BaSO_4$ was used as the reference. The spectra were transformed into the Kubelka-Munk function and subsequently deconvoluted into subbands by standard peak-fitting software[1].

Infrared spectra of about 1 mg of zeolite diluted in approximately 100 mg of KBr were recorded on a Nicolet Avatar 360 spectrometer.

Low- and high-angle XRD spectra were recorded on a Bruker D4 Endeavor powder diffraction system using Cu Kα radiation in the range $0.5\ ^\circ \leq 2\theta \leq 10\ ^\circ$ with a scanning speed of $0.0057\ ^\circ\ min^{-1}$ (small angle) and in the range of $5\ ^\circ \leq 2\theta \leq 50\ ^\circ$ with a scanning speed of $0.01\ ^\circ\ min^{-1}$ (high angle).

Nitrogen sorption isotherms were determined at -196 °C on a Micromeritics ASAP2020 system in static measurement mode. The samples were outgassed at 400

°C for 8 h prior to the sorption measurements. The Brunauer-Emmett-Teller (BET) model was applied to calculate the total surface area (S_{BET}) from the adsorption data obtained (p/p_0= 0.05-0.20). The mesopore volume ($V_{mesopore}$) and mesopore size distribution was calculated from the adsorption branch of the isotherm by the Barrett-Joyner-Halenda (BJH) method. The micropore and mesopore volumes were discriminated by the *t*-plot method employed at thicknesses between 3.5 and 5 Å. The mesopore volume and surface area contain contributions from the mesopores, macropores and the outer surface of the particles.

Transmission electron micrographs (TEM) were acquired on a FEI Tecnai 20 at an acceleration voltage of 200 kV. Typically, a small amount of catalyst was suspended in ethanol, sonicated and dispersed over a Cu grid with a holy carbon film. Scanning electron microscopy (SEM) was undertaken on a FEI Quanta 200F scanning electron microscope operating at an accelerating voltage of 1-30 kV.

Raman spectra were recorded at room temperature by a Jobin-Yvon T64000 triple-stage spectrograph with spectral resolution of 2 cm-1. The 290 nm laser line from a Coherent Innova 300 Fred laser was used as the excitation source. The power of the 290 nm line at samples was below 1.0 mW.

Stoichiometric nitrous oxide decomposition was carried out by first calcining a known amount of catalyst in artificial air (20 vol.% O_2 in He) at 550 °C (ramp rate 2 °C/min), followed by cooling in He to 250 °C at a rate of 5 °C/min. The reactor flow was then changed from He (80 Nml/min) to a mixture of 0.98 vol.% N_2O and 0.97 vol.% Ar in He (50 Nml/min) at 250 °C. The effluent flow was measured by a well-calibrated mass-spectrometer (Balzers Omnistar). The amount of nitrous oxide which was decomposed by the Fe^{2+} sites was computed from the amount of N_2.

The amount of coke deposits was estimated by temperature programmed oxidation of spent catalysts (after 24 h time on stream in benzene hydroxylation). To this end, the spent catalyst was exposed to a flow of 6 vol.% O_2 in He at a total flow rate of 100 Nml/min. The temperature was raised from room temperature to 700 ºC at a rate of 10 ºC/min. The amount of CO_2 was quantified by a Balzers mass-spectrometer. The CO_2 (m/*e* = 44) signal was calibrated by the thermal decomposition of a known amount of $NaHCO_3$.

Reactivity measurements

The catalytic performance of the zeolites in the oxidation of benzene to phenol with nitrous oxide was evaluated in a quartz plug flow reactor.[2] Typically, 0.1 g of zeolite catalyst with a sieve fraction of 125-425 μm was mixed with silicon carbide of the same sieve fraction and retained between quartz wool plugs. Benzene was

introduced into a gas flow of nitrous oxide and helium via a liquid mass flow controller and a controlled evaporator mixer (Bronkhorst). The final reactant feed mixture consisted of 1 vol.% benzene and 4 vol.% nitrous oxide in He at a total flow rate of 100 Nml/min . The gas hourly space velocity was 30,000 h^{-1}. The valves and most tubing of the reaction system were placed in an oven held at 180 °C to avoid condensation of phenol and other heavy product molecules. The gas phase composition was determined by a combination of online gas chromatography (Hewlett-Packard GC-5890 equipped with an HP-5 column and a flame ionization detector) and mass spectrometry (Balzers TPG-215). The reaction products included phenol, water, carbon monoxide, and carbon dioxide. The nitrous oxide and benzene conversions, nitrous oxide selectivity (fraction of oxygen atoms from nitrous oxide incorporated in phenol) and benzene selectivity (fraction of benzene converted to phenol) and the reaction rate of phenol were calculated. The carbon and nitrogen mass balances closed at 98% after prolonged reaction time.

Results

UV-Vis spectroscopy

Fig. S1 displays the UV-Vis spectra of the conventional Fe/ZSM-5 zeolites. The spectrum of the as-synthesized zeolite (Fe/ZSM-5-as), is dominated by two characteristic oxygen-to-metal charge-transfer (CT) bands for Fe^{3+} around 211 and 245 nm, which are characteristic for Fe^{3+} at isolated tetrahedral framework sites. After calcination the CT maximum of Fe/ZSM-5-cal shifted slightly to higher wavelengths, which may indicate the migration of part of the Fe^{3+} ions from framework to extraframework positions. After steaming, the spectrum of Fe/ZSM-5-S further shifted to higher wavelengths. Typical *d-d* transitions of Fe^{3+} in tetrahedral coordination in the zeolite framework are also visible. These transitions largely disappear upon calcination and steaming in line with our earlier work.[1] To follow these changes in more detail, the UV-Vis spectra were deconvoluted into various subbands. Two CT bands were used below 260 nm for isolated Fe^{3+} species and four bands at fixed wavelengths of 277, 333, 427 and 545 nm for isolated octahedral Fe^{3+} complexes, octahedral Fe^{3+} in oligomeric clusters, larger Fe_2O_3-like aggregates and bulk iron oxides, respectively.[3] The corresponding fit results are collected in Table S1. Fig. S2 displays the UV-Vis spectra of the hierarchical Fe/ZSM-5 zeolites. The trends are similar to those observed for Fe/ZSM-5. The *d-d* transitions, however, are much weaker which indicates that the fraction of iron ions in the zeolite framework is lower. UV-Vis spectra of mesoFe/ZSM-5-as and mesoFe/ZSM-5-ex are quite similar, indicating that the extraction process did not change the coordination environment of

Fe species. Correspondingly, the UV-Vis spectra of calcined mesoFe/ZSM-5-as and calcined mesoFe/ZSM-5-ex are quite similar. This also holds for the steamed materials. These qualitative results are supported by the results of the deconvolution of the UV-Vis spectra. Compared to Fe/ZSM-5, the as-synthesized hierarchical zeolite contains less isolated Fe^{3+} ions in line with the lower intensity of the *d-d* transitions. The as-synthesized hierarchical zeolite also contains a fraction of oligomeric octahedral Fe^{3+} clusters. Calcination and steaming result in a further loss of the Fe^{3+} dispersion. The final Fe speciation of the calcined and steamed hierarchical Fe/ZSM-5 zeolites differs only slightly from that in the corresponding conventional zeolites. The former zeolites contain a somewhat less dispersed iron oxide phase.

UV-Raman spectroscopy

UV resonance Raman spectroscopy is employed to characterize transition metal ions in the framework of zeolites and mesoporous silicas.[4-7] By using excitation in the UV region of the spectrum, fluorescence interference is minimized. The strong resonance Raman enhancement allows for the detection of small amounts of Fe in the framework of ZSM-5. The 290 nm excitation laser line is close in energy to the CT band which is dominant in the UV-Vis spectra. Fig. S3 displays UV-Raman spectra of Fe/ZSM-5-S and mesoFe/ZSM-5-ES catalysts. The band at 378 cm^{-1} is due to the symmetric stretching modes of Si-O-Si bonds and indicative of silicate frameworks containing five-membered rings.[8] Beside characteristic bands of the MFI structure at 290, 380, 460 and 800 cm^{-1},[8] the UV Raman spectra exhibit bands at 516, 1016, 1115, and 1165 cm^{-1}. The bands at 516 and 1115 cm^{-1} are assigned to the symmetric and asymmetric stretching vibrations of the framework Fe-O-Si species, respectively.[6,8,9] They can be observed despite the relatively low Fe concentrations in the samples due to the resonance Raman effect. The band at 1165 cm^{-1} is due to the Fe-O stretching vibration and is connected to the stretching of four neighboring framework Si-O-Si bonds.[10] The UV Raman results strongly suggest that the presence of the Fe species located in the crystalline environment in zeolite structures for the mesoFe/ZSM-5 catalysts. Compared with Fe/ZSM-5,[8] the steam-calcined catalysts do not have a prominent band at 1165 cm^{-1}. This indicates that the concentration of framework Fe species is very low. The migration of framework species into extraframework positions is in agreement with the UV-Vis spectroscopic results.

FT-IR spectroscopy

Fig. S4 displays the infrared spectra in the region of the silicate vibrations of conventional and hierarchical Fe/ZSM-5 catalysts. The relative crystallinity was

estimated from $(I_{550}/I_{450})/0.72 \times 100\%$ with I_{550} and I_{450} being the intensities of the infrared bands near 550 and 450 cm^{-1}.[11] These bands are related to the characteristic vibration of the double-five ring in MFI zeolite and the Si-O vibration, respectively. The high crystallinity of the various zeolite catalysts is confirmed by values above 90% for all catalysts.

High-angle XRD

Fig. S5 displays high-angle XRD spectra of conventional and hierarchical Fe/ZSM-5 catalysts. The patterns evidence the presence of crystalline zeolites with the MFI topology. No typical diffraction peaks due to large iron oxide aggregates were observed in the XRD patterns. The crystallinity from XRD was defined[12] as the ratio of the sum of the heights of the four most intense reflections in the region 2θ = 22.5-24º of the sample and the corresponding sum of a HZSM-5 reference zeolite (Akzo Nobel, Si/Al = 19.4). The XRD crystallinity is summarized in Table S2. The crystallinity for the hierarchical zeolites estimated from XRD is much lower (50-60%) than the values estimated from FTIR (>90%). This difference suggests that the microporous domains are quite small.

Small-angle XRD

Fig. S6 displays small-angle XRD spectra of hierarchical Fe/ZSM-5 catalysts. The absence of pronounced small-angle reflections in the XRD pattern indicates the lack of an ordered arrangement of the mesopores.

Nitrogen sorption

Fig. S7 displays nitrogen sorption isotherms of conventional and hierarchical Fe/ZSM-5 catalysts. The isotherm of Fe/ZSM-5-S is of type I, which is typical for microporous zeolites. The uptake at high relative pressure ($p/p_0 > 0.9$) results from the interparticle voids. The isotherms of mesoFe/ZSM-5-E, mesoFe/ZSM-5-ES and mesoFe/ZSM-5-S are a mixture of type I and type IV isotherms. The hysteresis loop in the range $0.4 < p/p_0 < 0.8$ shows the existence of mesopores in these materials. The sharp uptake at relative pressure $p/p_0 < 0.05$ confirms the presence of micropores. The textural properties show that mesoFe/ZSM-5 zeolites contain both micropores and mesopores. The mesopore volume, V_{meso}, decreases in the order mesoFe/ZSM-5-E ≈ mesoFe/ZSM-5-ES > mesoFe/ZSM-5-S > Fe/ZSM-5-S.

Fig. S8 displays BJH mesopore size distributions of the various catalysts. The mesopores in the various materials are not uniform in size. The amount of mesopores in Fe/ZSM-5-S is limited. The HK micropore size distributions (not shown) predict

micropores in the order of 5 Å for all materials.

Scanning electron microscopy

Fig. S9 shows secondary electron micrographs of conventional and hierarchical Fe/ZSM-5 catalysts. Fe/ZSM-5-S has a quite uniform morphology and the crystallite size is about 300-500 nm as reported before.[1] The hierarchical Fe/ZSM-5 zeolite (mesoFe/ZSM-5-E and mesoFe/ZSM-5-ES) exhibits a rather uniform globular morphology and quite large particle size (2-3 μm). Bulk zeolite crystals similar to those encountered in the micrographs of Fe/ZSM-5-S were not found.

Stoichiometric nitrous oxide decomposition

Fig. S10 displays a typical example of the stoichiometric decomposition of nitrous oxide. Upon switching the gas flow from He to N_2O/He, part of the nitrous oxide feed is decomposed into N_2. There is no evolution of molecular oxygen. From the amount of evolved N_2, the number of Fe^{2+} sites which can be reoxidized by N_2O was computed.

Determination of amount of carbonaceous material

Fig. S11 compares the evolution of the amount of CO_2 for various zeolites. The amount of carbonaceous deposits was estimated from the amount of carbon evolved by calibration against a $NaHCO_3$ standard. The quantitative results are given in Table 1.

Benzene hydroxylation

Table S3 compares the benzene conversion and phenol selectivity, nitrous oxide conversion and selectivity for Fe/ZSM-5-S and mesoFe/ZSM-5-ES as a function of reaction time. For Fe/ZSM-5-S, the phenol selectivity increases with decreasing conversion, as reported previously.[1] In contrast, the phenol selectivity of mesoFe/ZSM-5-ES decreases slightly with decreasing conversion. The lower selectivities go with increased formation of CO_x and H_2O which is the result of deep oxidation reactions. The decreasing nitrous oxide selectivities have been related before to the increasing contribution of combustion of coke deposits.[1]

Literature

1. E.J.M. Hensen, Q. Zhu, R.A.J. Janssen, P.C.M.M. Magusin, P.J. Kooyman, R.A. van Santen, *J. Catal.*, 2005, **233**, 123.
2. Q. Zhu, R.M. van Teeffelen, R.A. van Santen, E.J.M. Hensen, *J. Catal.*, 2004, **221**, 575.
3. S. Bordiga, R. Buzzoni, F. Geobaldo, C. Lamberti, E. Giamello, A. Zecchina, G. Leofanti, G. Petrini, G. Tozzola, G. Vlaic, *J. Catal.*, 1996, **158**, 486.
4. P.C. Stair, *Adv. Catal.*, 2007, **51**, 75.
5. C. Li, *J. Catal.*, 2003, **216**, 203.
6. C. Li, *Stud. Surf. Catal. Sci.*, 2007, **170**, 561.
7. L. Zhang, H.C.L. Abbenhuis, G. Gerritsen, N. Ni Bhriain, P.C.M.M. Magusin, B. Mezari, W. Han, R.A. van Santen, Q.H. Yang, C. Li, *Chem. Euro. J.*, 2007, **13**, 1210.
8. F.T. Fan, K.J. Sun, Z.C. Feng, H.A. Xia, B. Han, Y.X. Lian, P.L. Ying, C. Li, *Chem. Euro. J.*, 2009, **15**, 3268.
9. Y. Yu, G. Xiong, C. Li, F.S. Xiao, *J. Catal.*, 2000, **194**, 487.
10. K.J. Sun, F.T. Fan, H.A. Xia, Z.C. Feng, W.X. Li, C. Li, *J. Phys. Chem. C*, 2008, **112**, 16036.
11. G. Coudurier, C. Naccache, J.C. Vedrine, *J. Chem. Soc., Chem. Commun.*, 1982, 1413.
12. R. Szostak, *Molecular Sieves*, Springer, 1997, p. 290.

Figures

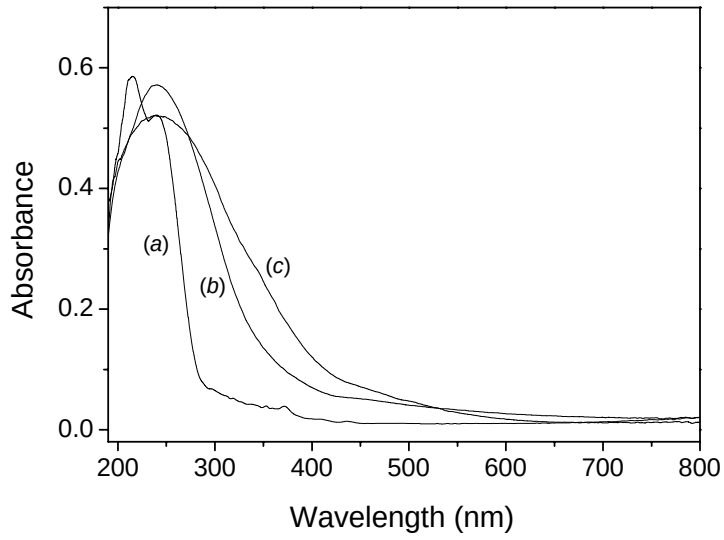

Fig. S1 UV-Vis spectra of conventional Fe/ZSM-5 catalysts: (a) Fe/ZSM-5-as, (b) Fe/ZSM-5-cal and (c) Fe/ZSM-5-S.

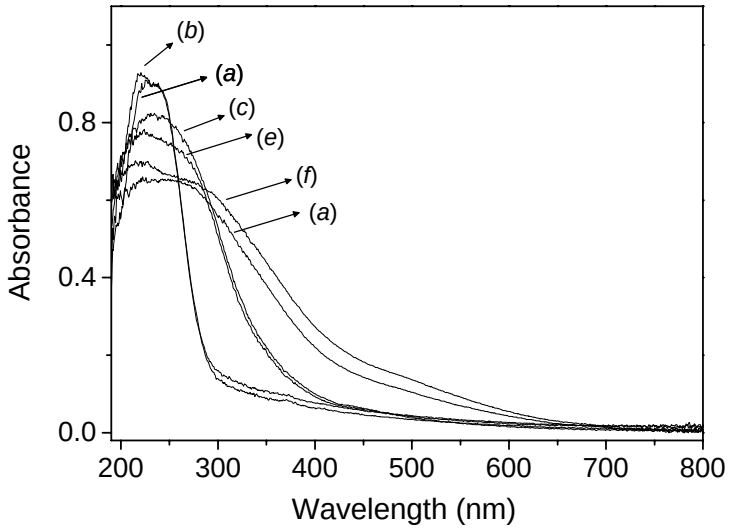

Fig. S2 UV-Vis spectra of hierarchical Fe/ZSM-5 catalysts: (a) mesoFe/ZSM-5-as, (b) mesoFe/ZSM-5-ex, (c) mesoFe/ZSM-5-cal, (d) mesoFe/ZSM-5-S, (e) mesoFe/ZSM-5-E and (f) mesoFe/ZSM-5-ES.

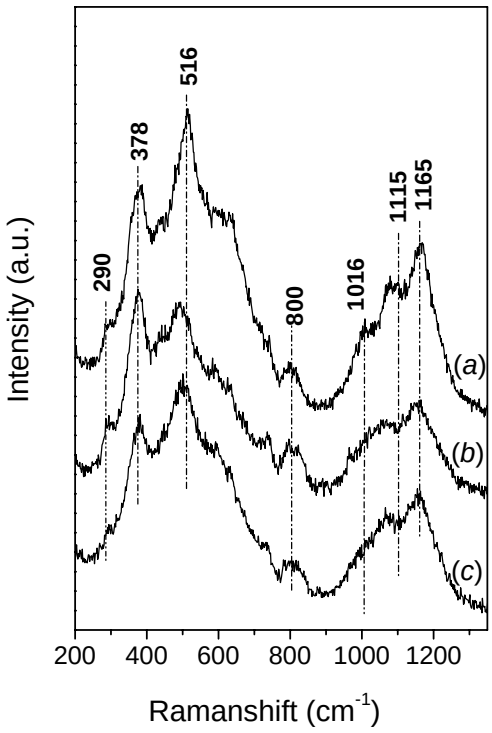

Fig. S3. UV resonance Raman spectra excited with a 290 nm laser of conventional and hierarchical Fe/ZSM-5 catalysts: (a) Fe/ZSM-5-S, (b) mesoFe/ZSM-5-ES and (c) mesoFe/ZSM-5-S.

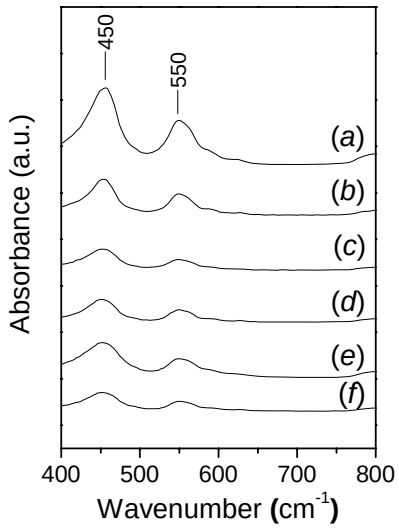

Fig. S4. FTIR spectra of conventional and hierarchical Fe/ZSM-5 catalysts: (a) Fe/ZSM-5-cal, (b) Fe/ZSM-5-S, (c) mesoFe/ZSM-5-E, (d) mesoFe/ZSM-5-ES, (e) mesoFe/ZSM-5-cal and (f) mesoFe/ZSM-5-S.

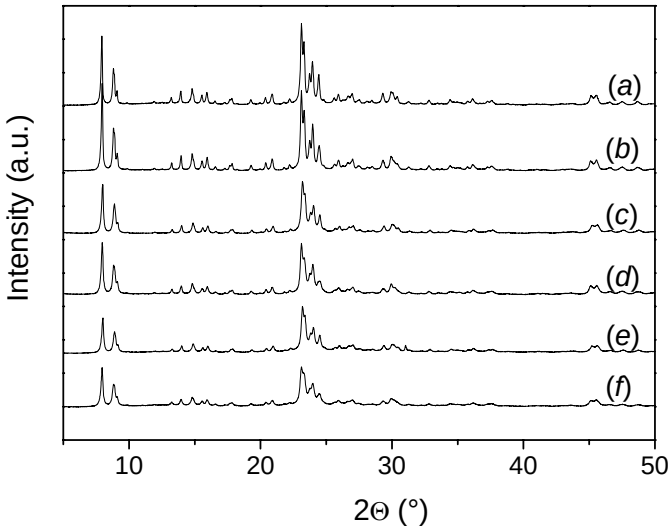

Fig. S5 High-angle XRD spectra of conventional and hierarchical Fe/ZSM-5 catalysts: (a) Fe/ZSM-5-cal, (b) Fe/ZSM-5-S, (c) mesoFe/ZSM-5-E, (d) mesoFe/ZSM-5-ES, (e) mesoFe/ZSM-5-cal and (f) mesoFe/ZSM-5-S.

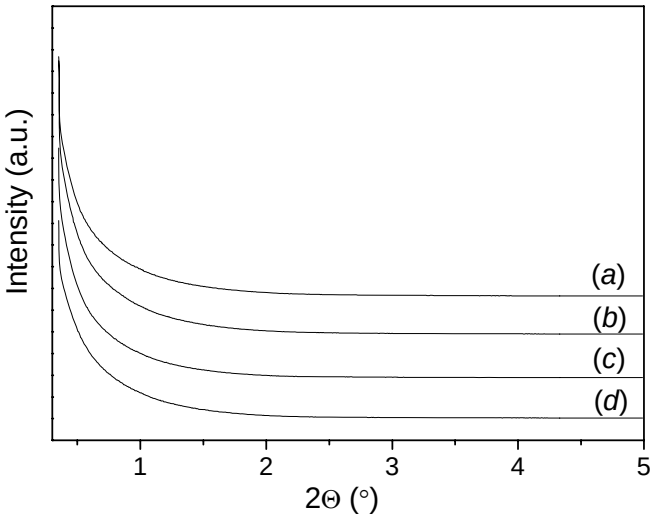

Fig. S6 Small-angle XRD spectra of hierarchical Fe/ZSM-5 catalysts: (a) mesoFe/ZSM-5-E, (b) mesoFe/ZSM-5-ES, (c) mesoFe/ZSM-5-cal and (d) mesoFe/ZSM-5-S.

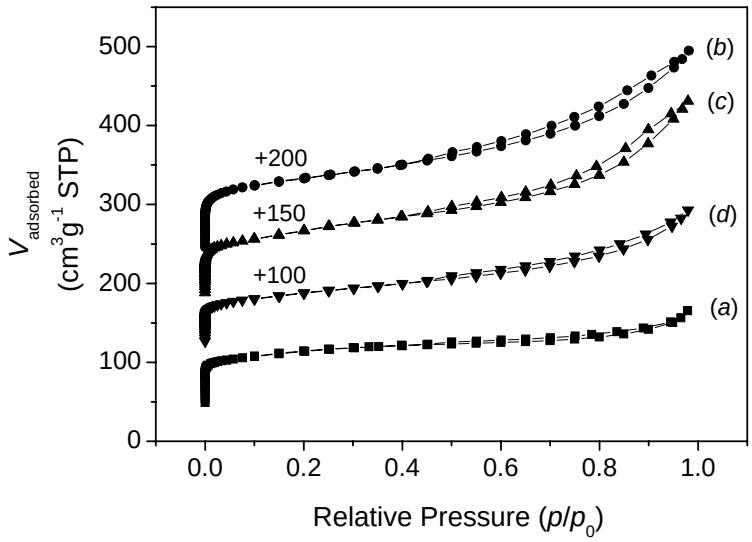

Fig. S7. Nitrogen sorption isotherms of conventional and hierarchical Fe/ZSM-5 catalysts: (a) Fe/ZSM-5-S, (b) mesoFe/ZSM-5-E, (c) mesoFe/ZSM-5-ES and (d) mesoFe/ZSM-5-S.

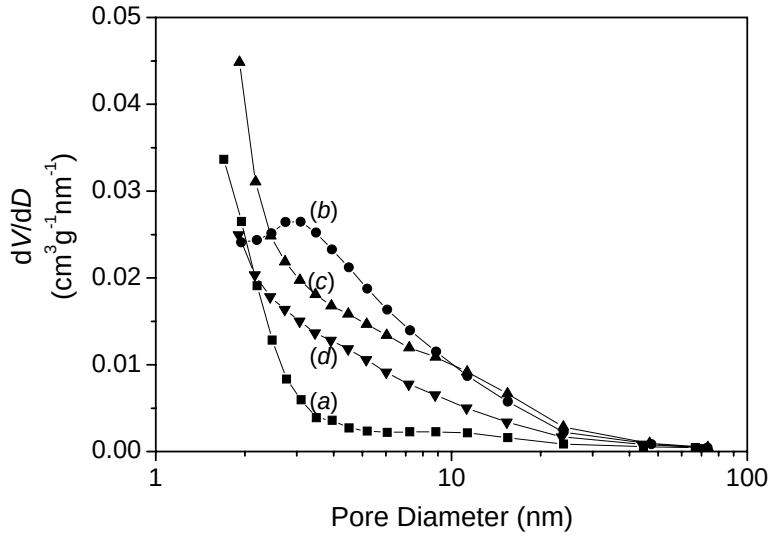

Fig. S8. BJH mesopore size distributions of conventional and hierarchical Fe/ZSM-5 catalysts: (a) Fe/ZSM-5-S, (b) mesoFe/ZSM-5-E, (c) mesoFe/ZSM-5-ES and (d) mesoFe/ZSM-5-S.

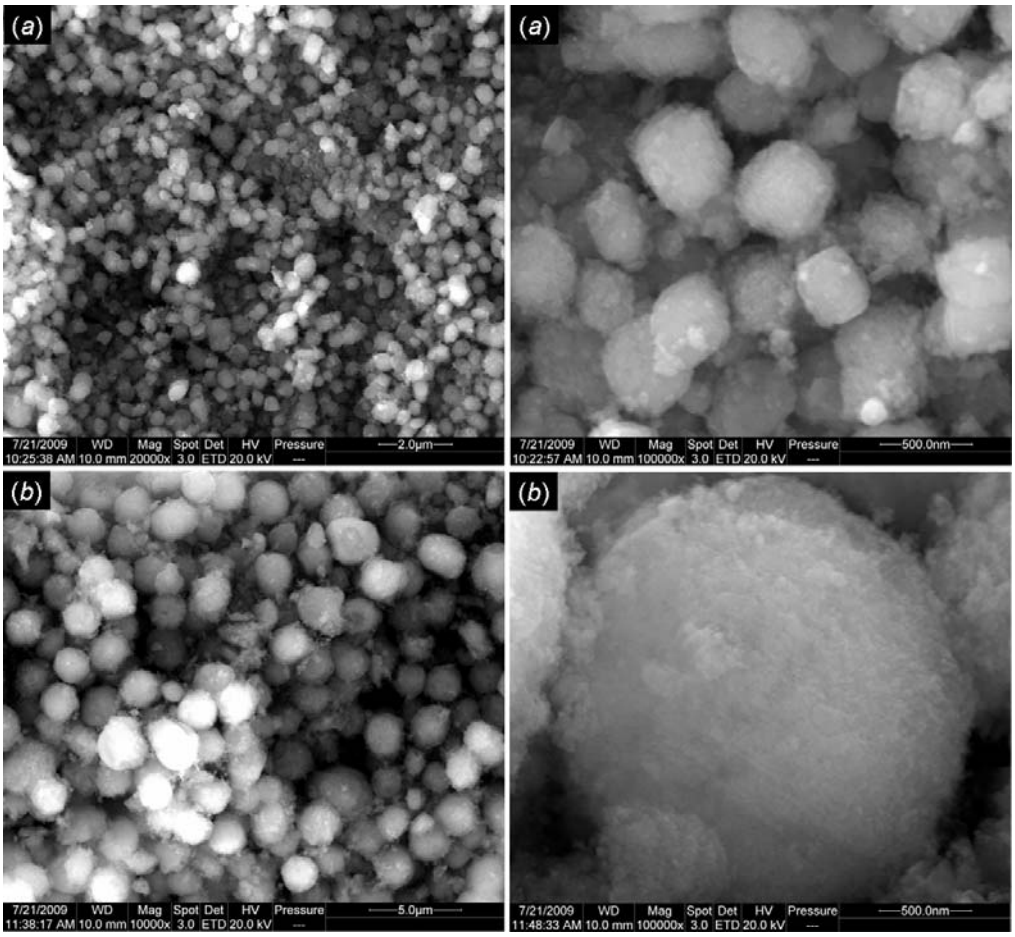

Fig. S9. Scanning electron micrographs of conventional and hierarchical Fe/ZSM-5 zeolites: (a) Fe/ZSM-5-S and (b) mesoFe/ZSM-5-ES.

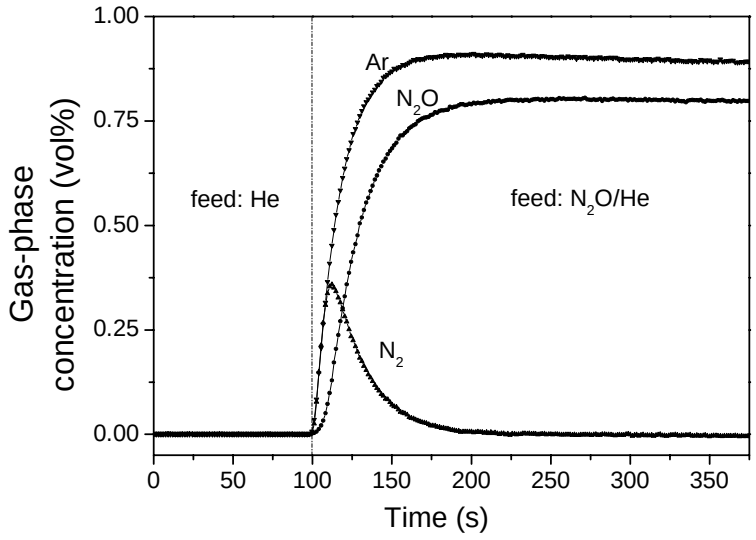

Fig. S10. Nitrous oxide decomposition of Fe/ZSM-5-S: response to a step change in the flow from He (80 Nml/min) to a mixture of 0.98 vol.% N_2O and 0.97 vol.% Ar in He (50 Nml/min) at 250 °C.

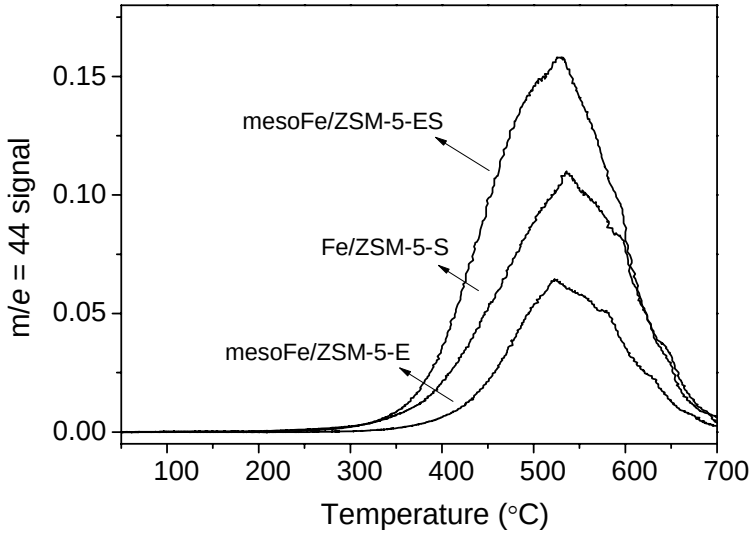

Fig. S11. Mass spectrometer signal of carbon dioxide upon calcination of spent catalyst.

Tables

Table S1. Contributions of subbands below 260 nm and at 277, 333, 427 and 545 nm from deconvolution of UV-Vis spectra of conventional and hierarchical Fe/ZSM-5 zeolites corresponding to Fig. S1 and Fig. S2.

Catalyst	I_λ<260 nm	I_λ=277 nm	I_λ=333 nm	I_λ=427 nm	I_λ=545 nm
Fe/ZSM-5-as	92	8	0	0	0
Fe/ZSM-5-cal	50	32	13	5	0
Fe/ZSM-5-S	41	24	24	9	2
mesoFe/ZSM-5-as	72	8	11	6	2
mesoFe/ZSM-5-ex	77	6	11	5	2
mesoFe/ZSM-5-E	49	31	15	5	2
mesoFe/ZSM-5-ES	34	19	27	13	7
mesoFe/ZSM-5-cal	44	35	15	5	1
mesoFe/ZSM-5-S	29	24	32	10	5

Table S2 Relative crystallinity estimated from infrared spectra and high-angle XRD spectra of conventional and hierarchical Fe/ZSM-5 zeolites.

Catalyst	IR crystallinity (%)	XRD crystallinity (%)
Fe/ZSM-5-cal	92	99
Fe/ZSM-5-S	96	97
mesoFe/ZSM-5-E	89	63
mesoFe/ZSM-5-ES	96	62
mesoFe/ZSM-5-cal	94	59
mesoFe/ZSM-5-S	102	51

The IR crystallinity[3] defined as $(I_{550}/I_{450})/0.72\times100\%$. I_{550} and I_{450} are the intensities of the infrared bands around 550 and 450 cm^{-1}, respectively. The XRD crystallinity[12] is defined as the ratio of the sum of the intensities of the four most intense reflections in the 2θ range of 22.5-24° and the corresponding sum for a crystalline HZSM-5 reference material (Akzo Nobel HZSM-5, Si/Al = 19.4).

Table S3. Reaction data for benzene hydroxylation by conventional and hierarchical Fe/ZSM-5 zeolites (reaction temperature 350 °C, feed composition: 1 vol% benzene, 4 vol% N_2O, 95 vol% He, GHSV 30,000 h^{-1}).

Catalyst		C_6H_6		N_2O		R_{phenol}
	Time	X (%)[1]	S (%)[2]	X (%)	S (%)	(mmol.g^{-1}.h^{-1})
Fe/ZSM-5-S	5 min	36	87	12	63	8.4
	1 h	17	81	5	74	3.8
	3 h	8	92	3	75	2.1
	5 h	6	98	2	73	1.5
	10 h	3	> 99	1	66	0.8
	24 h	< 1	-	1	35	0.4
mesoFe/ZSM-5-ES	5 min	45	> 99	18	70	12
	1 h	30	> 99	12	77	8.1
	3 h	25	94	10	62	6.4
	5 h	24	83	9	58	5.3
	10 h	20	74	7	54	3.9
	24 h	12	74	4	58	2.4

[1] Conversion; [2] Selectivity.